Multiproxy tree-ring reconstruction of glacier mass balance: Insights from *Pinus cembra* trees growing near Silvretta glacier (Swiss Alps)

Jérôme Lopez-Saez[1], Christophe Corona[1,2], Lenka Slamova[1,3], Matthias Huss[4,5,6], Valérie Daux[7], Kurt Nicolussi[8], Markus Stoffel[1,3,9],

[1]Climate Change Impacts and Risks in the Anthropocene (C-CIA), Institute for Environmental Sciences, University of Geneva, Geneva, Switzerland
[2] Université Grenoble Alpes, CNRS LECA, F-38000 Grenoble, France
[3]Department F.-A. Forel for Environmental and Aquatic Sciences, University of Geneva, Geneva, Switzerland
[4]Laboratory of Hydraulics, Hydrology and Glaciology (VAW), ETH Zurich, Zurich, Switzerland
[5]Swiss Federal Institute for Forest, Snow and Landscape (WSL), Birmensdorf, Switzerland
[6]Department of Geosciences, University of Fribourg, Fribourg, Switzerland
[7]Laboratoire des Sciences du Climat et de l'Environnement, LSCE/IPSL, CEA-CNRS-UVSQ, Université Paris-Saclay, Gif-sur-Yvette, France
[8]Institute of Geography, University of Innsbruck, Austria
[9]Department of Earth Sciences, University of Geneva, Geneva, Switzerland

Correspondence to: Jérôme Lopez-Saez (jerome.lopez-saez@unige.ch)

Abstract. Glacier mass-balance reconstructions provide a means of placing relatively short observational records into a longer-term context. Here, we use multiple proxies from *Pinus cembra* trees from God da Tamangur combining tree-ring anatomy and stable isotope chronologies to reconstruct seasonal glacier mass balance (i.e., winter, summer and annual mass balance) for the nearby Silvretta glacier over the last two centuries. The combination of tree-ring width, radial diameter of earlywood cell lumina and latewood radial cell wall thickness provides a highly significant reconstruction for summer mass balance, whereas for winter mass balance, correlation was less significant but still robust when radial cell lumina were combined with $\delta^{18}O$ records. Combination of the reconstructed winter and summer mass balances allows quantification of the annual mass balance of the Silvretta glacier, for which *in-situ* measurements date back to 1919. Our reconstruction indicates a substantial increase in glacier mass during the first half of the 19th century and an abrupt termination of this phase after the end of the Little Ice Age. Since the 1860s, negative glacier mass balances have been dominant and mass losses accelerate as anthropogenic warming picks up in the Alps.

1 Introduction

One of the most iconic and noticeable consequence of anthropogenic climate change at high elevations is the decrease of snow cover and the mass loss of glaciers (Zemp et al., 2019; Beaumet et al., 2021). In the European

Alps, glaciers have been retreating since the end of the Little Ice Age (c. 1850 CE) (Zemp et al., 2006) and future ice volumes are predicted to be largely reduced (Marzeion et al., 2018; Rounce et al., 2023), with ice losses of alpine glaciers reaching up to 90% by 2100 (Zekollari et al., 2019; Vincent et al., 2019). The ongoing reduction of glacier volumes has very direct, negative implications for water resources, ecosystems and livelihoods (IPCC, 2022; Huss and Hock, 2018; Immerzeel et al., 2020; Cauvy-Fraunié and Dangles, 2019; Bolibar et al., 2020).

Glaciers stand as one of the most important freshwater resources for societies and ecosystems. The recent increase in ice melt directly contributes to altered runoff patterns and rising sea levels (Anon, 2021). Recognizing their significance, the Global Climate Observing System (GCOS, https://gcos.wmo.int/en/home) has designated glaciers as an Essential Climate Variable (ECV). To reduce uncertainties in the quantification of future mass losses and their potential consequences, information on past glacier variability and changes is essential as it allows improving simulations of glacier evolution (e.g., Brunner et al., 2019). *In-situ* measurements of glacier mass balance constitute a key element in worldwide glacier monitoring. Open-access historical datasets – like those available from the World Glacier Monitoring Service (WGMS, 2021) – are crucial for an improved understanding of the glacier mass change and the calibration of models used for projections. The (net) mass balance of a glacier surface is defined as the difference between winter accumulation and summer ablation and is generally acknowledged as the prime variable of interest to monitor and project the state of glaciers and their hydrological contribution under global warming scenarios (Hock and Huss, 2021). However, only few glaciers around the world have long-term, direct mass balance observations as these measurements require considerable manpower, time, and economic resources to be sustained for a meaningful period of time (Kinnard et al., 2022). Despite recent monitoring efforts, the WGMS database – with more than 200 glacier mass balance series worldwide – contains only few records exceeding 20 years.

Various approaches have been used over the last decades to estimate mass balance over multi-decadal timescales, often relying on remotely sensed data. Studies included the use of gravimetry (e.g., Wouters et al., 2019), the interpretation of series of multiple Digital Elevation Models (e.g., Dussaillant et al., 2019), altimetry (e.g., Gardner et al., 2013) or glacier length change observations (e.g., Hoelzle et al., 2003). Whereas these approaches provided insights into past changes, the temporal resolution of results does not provide information on the inter-annual variability and the drivers of change in glacier mass balance. Mass balance modelling based on meteorological series (Huss et al., 2008; Nemec et al., 2009) allows to infer glacier mass balance over longer timescales at high temporal resolution. However, accurate modeling requires long records of temperature and precipitation from high elevation meteorological stations that are, in addition, located at the vicinity of the glaciers, but such datasets are scarce. To address this limitation, meteorological series are generally scaled to the glacier sites (Huss et al., 2021). While air temperature often show strong correlation over large distances (Begert et al., 2005), allow for confident extrapolation, it is more difficult to estimate the distribution of precipitation in alpine environments and larger uncertainties therefore persist in winter mass balance reconstructions (Sold et al., 2016).

High-elevation tree-ring proxies portray past summer temperature fluctuations and changes and – to a lesser extent – a winter precipitation signals; or, in other words, the main drivers of glacier fluctuations. Tree-ring proxies located at high-elevation sites and at the vicinity of glaciers, should thus hold the potential to extend glacier mass balance series farther back in time and offer an interesting alternative to meteorological series for mass balance reconstructions.

Several dendrochronological studies have been developed to test this hypothesis and have demonstrated the reliability of these proxies as reliable recorders of past mass balance variations. In the 2000s, seminal papers used tree-ring width (TRW) series to reconstruct mass balance patterns for glaciers in Canada (Lewis and Smith, 2004; Larocque and Smith, 2005; Watson et al., 2006). Since 2007, multiproxy mass balance reconstructions combining TRW with maximum latewood density (MXD), stable isotopes or Blue Intensity (BI) have been developed for glaciers in Pacific North America (Wood et al., 2011; Malcomb and Wiles, 2013), Scandinavia (Linderholm et al., 2007; Hiemstra et al., 2022) or Central Asia (Zhang et al., 2019) (see Tab. 1 for a complete review).

Reference	Location	Lat	Long	Mass Balance Reconstruction			Period	Nb of trees
				Winter	Summer	Annual		
Nicolussi and Patzelt, 1996	Gepatschfemer, Tyrol, Austria	46°84 N	10°75 E	EW (TRW)	LW (TRW)	EW + LW (TRW)	1400-1987	/
Lewis and Smith 2004	Vancouver Island, British Columbia, Canada	49°40 N	125°40 W			TRW	1412-1998	53
Larocque and Smith 2005	Mt Waddington, British Columbia, Canada	62°01 N	144°32 W	TRW	TRW	TRW	1550-2000	/
Watson et al., 2006	Peyto Glacier, Canada			TRW	TRW	TRW	1673-1994	74
Linderholm et al 2007	Storglaciären, Sweden	67°55 N	18°35 E	Circulation indices	TRW + MXD	Circulation indices+TRW + MXD	1780-1981	/
Wood et al 2011	Place Glacizer, British Columbia, Canada	50°25 N	122°36 W	MXD + TRW	TRW		1585-2006	61
Malcomb and Wiles 2013	Various glaciers, USA and Canada	47° N	123° W			TRW +LW + MXD	1500-1999	/
Shekhar et al 2017	Various glaciers Western Himalayan, India	32° N	77° E			TRW	1615-2015	189
Zhang et al, 2019	Tuyuksuyskiy Glacier, Kazakhstan	43°03 N	77°05 E	TRW	Stable isotope	TRW + stable isotope	1850-2014	50
Cerrato et al., 2020	Careser Glacier, Italy	46°25 N	10°41 E	Precipitation records	MXD	Precipitation records + MXD	1811-2013	24
Hiemstra et al., 2022	Jotunheimen, Norway	61°6 N	8°3 E	Precipitation records	BI	Precipitation records + BI	1722-2017	32

Table 1. *Synthesis of existing dendroclimatic studies, tree-ring proxies as well as meteorological data used for the reconstruction of winter (B_w), summer (B_s) and annual (B_a) glacier mass balance.*

In the Alps, mass balance reconstructions are much scarcer: Nicolussi and Patzelt (1996) reconstructed 600 years of glacier mass balance for the Gepatschferner glacier using TRW records. More recently, both summer and winter mass balance back to 1811 CE have been reconstructed for the Careser glacier in Italian Alps (Cerrato et al., 2020) with maximum latewood density (MXD) and long meteorological series available for the Alpine region (Brunetti et al., 2006, 2012, 2014; Crespi et al., 2018).

In Switzerland, GLAMOS (GLAcier Monitoring Switzerland; www.glamos.ch) hosts a complete compilation of measured and re-analyzed mass balance data of Swiss glaciers, of which several span much of the 20th century (Huss et al., 2015). Despite the uniqueness of these records and their potential for validation and calibration of proxy-based reconstructions, no attempts have been undertaken so far to extend these datasets beyond the 20th century or even to preindustrial times.

In addition, recent developments in quantitative wood anatomy (QWA), relying on the analysis of dimensions of wood cells in tree-rings, demonstrated that this approach offers an unparalleled measurement precision and substantial gain in temperature reconstructions (Lopez-Saez et al., 2023; Seftigen et al., 2022; Allen et al., 2022; Björklund et al., 2023). In this context, the aim of this study is to assess the reliability of a multiproxy approach, using only tree-ring proxies, in extending historical winter and summer mass balance series farther into the past. To reach this goal, we employed stable isotope ($\delta^{18}O$, $\delta^{13}C$) and tree-ring anatomy chronologies of *P. cembra* which has recently been shown to be very sensitive to mean temperature over the ablation season (April–September; Lopez-Saez et al., 2023). We selected the Silvretta glacier in the Eastern Swiss Alps as our study site due to the availability of glacier mass balance data spanning from 1920 to present, making it one of the longest continuous series in the Alps. Using increment cores from trees growing close to the Silvretta glacier, we (i) construct TRW, anatomical and isotope chronologies to (ii) derive annual time series of past summer temperature and winter precipitation as proxies of summer and winter glacier mass balance. Our reconstruction provides new insights into mass balance dynamics of an Alpine glacier during the maximum and the termination of the Little Ice Age, a phase of important dynamics in glacier evolution but very limited direct evidence on the rates and the exact timing of changes.

2 Materials and methods

2.1 Glacier and tree-ring sites

The study focuses on the Eastern Swiss Alps, close to the borders with Austria and Italy (Fig. 1A). Silvretta (46.85° N; 10.08°E) is a small temperate mountain glacier with a surface area of presently 2.7 km^2 extending from 3,070 down to 2,470 m asl (Fig. 1A, B). The mean equilibrium line altitude of Silvretta was 2775 m a.s.l. between 1960 and 1990 with a standard deviation of 140 m and its first mass balance measurements date back to 1919 CE. Seasonal observations at two stakes were conducted until 1959, when the stake network was increased to 40 stakes. Today, 18 stakes are surveyed seasonally. Huss et al. (2009) re-analyzed and homogenized the seasonal stake data back to 1959.

Silvretta is a global reference glacier of the WGMS and the monitoring is maintained in the frame of GLAMOS. The tree-ring site is located c. 30 km to the southeast of Silvretta glacier and known locally as God da Tamangur (46.68°N; 10.36°E) – meaning the « forest back there» in Vallader Romansch. It is the highest, pure, and continuous *P. cembra* forest in Europe (Fig. 1A, C). The forest is located at an elevation of up to 2,300 m asl, at the end of Val S-charl (Grisons, Switzerland), on the NW-facing slope of Piz Starlex (3,075 m asl). Lopez-Saez et al. (2023) recently showed that various wood anatomical parameters extracted from this forest allow robust reconstruction of past temperature variability at annual to multidecadal timescales.

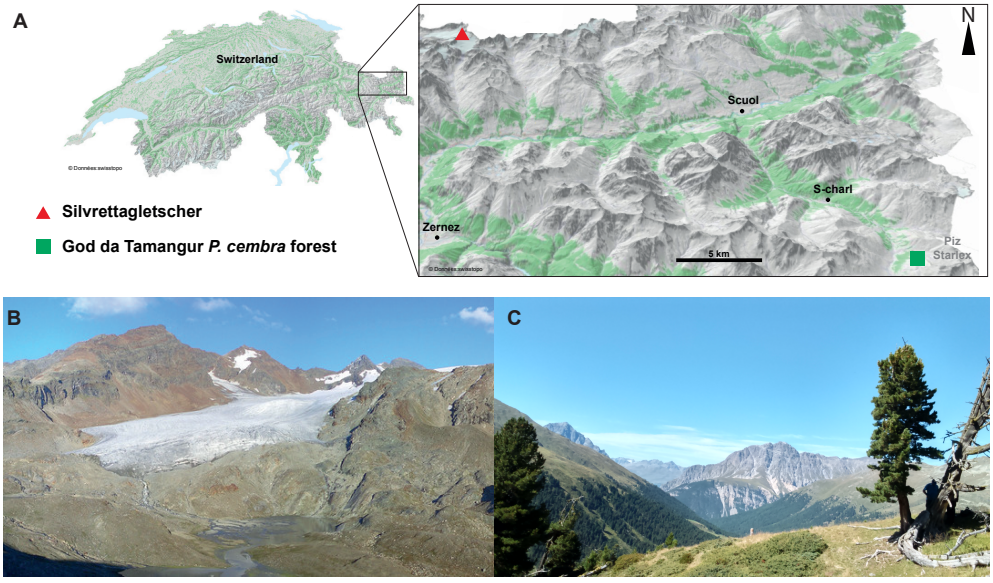

Figure 1. *(A) The study site is in the eastern part of Switzerland, close to the municipality of Scuol. (B) Overview of the Silvretta glacier (www.glamos.ch) and (C) detailed view of a century-old P. cembra tree from God da Tamangur (Val S- charl, Scuol, Grisons, Switzerland) selected for analysis.*

2.2 Sample collection and wood processing

Tree cores were collected during a field campaign in summer 2018. To perform TRW analyses, 46 trees were sampled using a 12 mm increment borer. From each tree, we extracted two increment cores at breast height (*c.* 130 cm above ground). Ring widths were measured to the nearest 0.01 mm using TSAPWin (Rinntech, Germany), cross-dated using standard dendrochronological procedures (Stokes and Smiley, 1996) and checked for dating and measurement errors with the COFECHA software (Holmes, 1983). Ring widths from single radii were summarized to mean widths per tree. Values from 20 individual trees showing the best TRW inter-series correlation

and covering the period 1802–2017 were averaged into a master TRW chronology to ensure consistent sample depth across time.

2.3 Wood anatomical analyses

To perform wood anatomical analyses, the first of the two sampled cores from each of the 20 individuals included in the master TRW chronology was split into 4–5 cm long pieces to obtain 15 µm thick cross-sections with a rotary microtome (Leica RM 2255/2245). The sections were stained with Safranin and Astra blue to increase contrast and fixed with Canada balsam following standard protocols (Gärtner and Schweingruber, 2013; von Arx et al., 2016). Digital images of the microsections - at a resolution of 2.27 pixels/µm - were produced at the Swiss Federal Research Institute WSL (Birmensdorf, Switzerland), using a Zeiss AxioScan Z1 (Carl Zeiss AG, Germany). For the 20 trees, we used the ROXAS (v3.1) image analysis software (von Arx and Carrer, 2014) to automatically detect anatomical structures for all tracheid cells and annual ring boundaries for the period 1800–2017. We excluded measurements of samples with cell walls damaged during sampling or preparation and focused on two parameters in quantitative wood anatomy analyses: radial cell lumen diameter (D_{rad}) and radial cell wall thickness (CWT_{rad}) (Prendin et al., 2017; von Arx and Carrer, 2014).

Following Lopez-Saez et al. (2023), we assigned each cell to tangential bands of 40 µm in radial width (with distances measured parallel to ring boundaries). In addition, we determined the transition from earlywood to latewood cells for each ring using Mork's index = 1, at a 10 µm radial resolution (Denne, 1989; see Lopez-Saez et al., 2023 for more details). For each ring, maximum values of D_{rad} and CWT_{rad} were extracted from the bands identified as belonging to the ring. For D_{rad}, maximum values were extracted from each ring in the earlywood. For CWT_{rad}, maximum values were extracted from the latewood.

2.4 Isotopic analyses

For the isotopic analyses ($\delta^{18}O$ and $\delta^{13}C$), we selected ten trees showing the best inter-series correlation out of the 20 trees used for TRW and QWA analyses. Selected samples were between 242 and 634 years old at the time of sampling. Cores were cut ring by ring with a scalpel at the Laboratoire des Sciences du Climat et de l'Environnement (LSCE, Gif-sur-Yvette, France). The wood from each ring was processed separately between 1968 and 2017 and every fifth year between 1802 and 1967, so that in total, 83 years were measured on each individual core. For all other years between 1802 and 1965, material from the ten trees of the same year was pooled prior to analysis. The wood samples were grounded and α-cellulose was extracted according to the SOXHLET chemical method (Leavitt and Danzer, 1993) and homogenized ultrasonically. The oxygen and carbon isotopic composition was obtained by high temperature pyrolysis in a high-temperature conversion elemental analyzer (Thermo Scientific) coupled to an Isoprime mass spectrometer (see Penchenat et al., 2022 for details). The

measured sample values were corrected based on an internal laboratory reference of cellulose (Whatmann® CC31) analyzed every three samples in each sequence of analysis. The analytical precisions of the instruments were within ±0.20‰ for $\delta^{18}O$ and ±0.10‰ for $\delta^{13}C$, respectively, based on the standard uncertainty of the mean. A correction to the $\delta^{13}C$ raw series was applied by means of linear interpolation to compensate for decreasing $\delta^{13}C$ in organic matter related to fossil-fuel combustion and increasing atmospheric concentration. The oxygen and carbon isotopic composition were expressed as δ following (Francey et al., 1999; McCarroll and Loader, 2004):

$$\delta = (R_{samp} – R_{VSMOW}\text{-}1) \times 1000$$

where R_{samp} is the isotopic ratio in the sample and R_{VSMOW} the isotopic ratio in the Vienna Standard Mean Ocean Water (for oxygen) or the Vienna Pee-Dee belemnite (for carbon) (Coplen, 1996).

2.5. Establishment of wood proxy chronologies

The conventional TRW measurements were detrended with a negative exponential function to eliminate non-climatic (e.g., age-related growth trends and other biological disturbances) effects from the series (Fritts, 1976; Cook and Kairiukstis, 1990). The detrended series were then aggregated into a TRW chronology using a biweight robust mean which reduces the influence of outliers (Cook and Peters, 1981). Given the absence of any evident long-term ontogenetic trend in anatomical series, detrending is not normally considered necessary (Carrer et al., 2018; Lopez-Saez et al., 2023) in QWA studies. As isotope chronologies were pooled prior to analysis, we did not detrend the data further. This absence of detrending has little influence on subsequent analyses as $\delta^{18}O$ only contains minor changes related to age (Torbenson et al., 2022) while the presence of age-related trends remains debated for $\delta^{13}C$ for which studies show age trends throughout the lifespan (Helama et al., 2015) but also the lack thereof (Büntgen et al., 2021).

In a next step, empirical measures of dendroclimatic signals (Hughes et al., 2011) were computed to test the strength of the environmental information embedded in each wood proxy chronology using the maximum overlap of pairwise correlations (Bunn et al., 2013). These included average inter-series correlation ($RBAR_{EFF}$) and expressed population signal (EPS) (Wigley et al., 1984). All analyses were performed in R Studio (R Studio Team, 2023) using the R package dplR (Bunn, 2008; Bunn et al., 2013).

2.6 Meteorological series

In this study, the gridded (1 × 1 km) daily mean temperature and precipitation time series available from Imfeld et al. (2023), hereafter referred to as *Imfeld23*, were used to both identify the main drivers of radial growth and to

reconstruct glacier mass balance fluctuations. The dataset (1763-2020) includes meteorological data rescued by various initiatives (Brugnara et al., 2020; Pfister et al., 2019; Brugnara et al., 2022) for the late 18th and early 19th centuries and systematic measurements available in Switzerland since 1864. Time series were initially checked and homogenized on a subdaily basis (following Brugnara et al., 2020). The dataset was then reconstructed at a 1 × 1 km resolution using an analogue method, which resamples meteorological fields for a historical period based on the most similar day in a reference period. The fields were improved with data assimilation for temperature and bias correction with quantile mapping for precipitation (Imfeld et al., 2023). Several limitations must be considered when working with this exceptional dataset: (1) the reconstruction skills decrease prior to 1864 as fewer stations provide direct observations, (2) larger reconstruction errors are observed for precipitation than for temperature due to the heterogeneous nature of precipitation, and (3) the quality of the dataset is spatially heterogeneous and considerably reduced in the Alps and the southern side of the Alps due to both the scarcity of observations and more complex topo-climatic conditions.

2.7 Climate–growth relationships

In a first step, we correlated wood proxy data with *Imfeld23* by selecting the grid point centered over the God da Tamangur study site. To test for the robustness of the mixed proxies series for climate–growth relationship, we calibrated regression models on temperature and precipitation averaged over 30 to 365-day windows starting on October 1 of the year preceding ring formation (n-1) and ending on September 30 of the year in which the ring was formed (n) using the R package DendroTools (Jevšenak and Levanič, 2018). This time window was chosen according to the growing season of *P. cembra* trees in the Alps (Saulnier et al., 2011). The selected time window encompasses both the accumulation and ablation periods, used to derive winter (October 1 – April 30) and summer (May 1 – September 30) mass balance series. Correlations were computed over the 1802-2017 period covered by the tree-ring proxy series.

2.8 Glacier mass balance multi-proxy reconstructions

In a next step, wood proxies correlated with precipitation totals and average air temperature during the ablation and accumulation periods were used as predictors to reconstruct winter (B_w) and summer (B_s) mass balance of the Silvretta glacier, respectively. Glacier-wide time series of winter and summer mass balance available for the Silvretta glacier (1919-2022) from the WGMS (Huss et al., 2015; WGMS, 2021) were used as predictands. Seasonal point measurements acquired in early May and September, respectively, were extrapolated to unmeasured areas of the glacier using a model-based extrapolation technique (Huss et al., 2015). Changes in the glacier geometry due to advance or retreat have a direct impact on the overall mass balance, mainly due to changes

in the elevation range. These effects are included in the observational dataset of glacier-wide mass balances as the latter always refer to the instantaneous glacier geometry. For the period before 1920, however, we do not explicitly adapt glacier geometry but assume the relations derived and tested over a 100-year period with significant changes to be representative.

A multiple linear regression model was selected for the reconstruction of winter and summer mass balances. When more than two proxies were included in the model, the number of predictors was lowered using principal component analysis. The first *n* principal components with eigenvalues exceeding 1 were retained in the principal component regression. We computed 10,000 summer and winter mass balance reconstructions using a split calibration–verification procedure coupled with a bootstrap approach in which 50% of the years covered by both the mass balance observation and wood-proxy datasets were randomly extracted for calibration while the remaining years were used for validation over the 1920-2017 period. For each sampling, the root mean-square error (RMSE), coefficient of determination (r^2 for the calibration and R^2 for the verification periods), reduction of error (RE) and coefficient of efficiency (CE) statistics (Cook et al., 1995) were applied to test the predictive capacity of the transfer function. Calibration and validation statistics are illustrated for each of the TRW, wood anatomical and isotope parameters with their 5^{th}, 50^{th} and 95^{th} percentiles. In a final step, annual mass balance (B_a) was reconstructed using the sum of the final winter and summer mass balance reconstructions.

In parallel, we reconstructed winter and summer mass balances over the 1763-2020 period using the gridded temperature and precipitation field records from *Imfeld23*. With the purpose to identify the optimal time window for the reconstruction, we selected the grid-point closest to the Silvretta glacier and calibrated regression models between daily temperature series computed over one-to-365-days windows starting on January 1 of the year preceding observations of summer mass balance and ending on December 31 of the year in which the mass balance measurement was acquired. In addition, daily precipitation-temperature series were used as regressors for observed winter-summer mass balances. For each optimal precipitation and temperature time window identified, we computed 10,000 reconstructions following the calibration/verification procedure described for tree rings.

3 Results and discussion

3.1 Isotope and wood anatomical features chronology characteristics

We measured wood anatomical features for the period 1802–2017 CE on the 20 sampled trees for a total of 75–100 radial files per ring, with anatomical information catalogued by its position in each dated tree ring. After the exclusion of cells with walls damaged during sampling or preparation, a total of 2,277,779 tracheid cells were used for analysis.

Fig. 2 showcases the evolution of wood anatomical parameters as a function of relative distance to ring border. It also shows that, based on Mork's index, latewood represents roughly 10% of total ring width on average. *P. cembra* trees feature the classical ring structure of conifers growing in cold, temperate environments, with an increase in radial cell wall thickness (CWT_{rad}, Fig.2A), and a monotonic reduction in radial diameter (D_{rad}, Fig. 2B), from earlywood to latewood. Statistical characteristics of the Tamangur chronologies are summarized in Tab. 2.

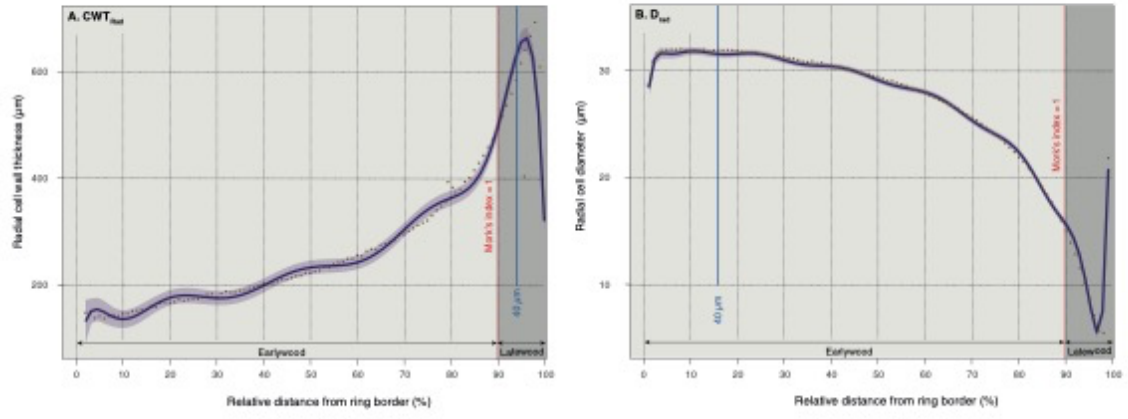

Figure 2. *Profiles of (A) radial cell-wall thickness (CWT_{rad}) and (B) radial cell diameters (D_{rad}) along P. cembra tree rings. Purple dots represent the mean values of twenty trees over 217 years (1800–2017) smoothed with a polynomial regression (black line) represented with its 95th confidence interval (shadowed purple areas). The blue line represents maximum values for each of the wood parameters analyzed for 40 µm wide radial bands. The red line shows the mean relative position of the transition between earlywood (light grey area) and latewood (dark grey area) according to Morck's index = 1.*

The EPS and Rbar values show that TRW has a stronger common signal (Rbar=0.39, EPS=0.85) than the wood anatomical chronologies (D_{rad}, CWT_{rad}), with the Rbar for the latter ranging between 0.16 (for D_{rad} at 40 µm radial band width) and 0.25 (for a CWT_{rad} at 40 µm radial band width). Several studies report lower common signals in wood anatomical parameters than in TRW series from deciduous (Fonti and García-González, 2004) and conifer trees (Seftigen et al., 2022).

Wood proxy	Bandwith (µm)	EPS	Rbar
Tree-ring width (TRW)		0.85	0.39
Radial diameter (D_{rad}) - Earlywood	40	0.75	0.16
Radial cell wall thickness (CWT_{rad}) - Latewood	40	0.84	0.25
δ13C (10-yr interval)		0.9	0.46
δ18O (10-yr interval)		0.91	0.48

285

Table 2. *Statistics of chronologies based on TRW, D_{rad}, CWT_{rad} and $\delta^{13}C$, $\delta^{18}O$ EPS = expressed population signal, Rbar = average inter-series correlation.*

This weaker signal is generally attributed to inter-annual variability in microscopic wood features (Olano et al., 2012;
290 Liang et al., 2013; Pritzkow et al., 2014), heterogeneous intra-annual internal physiological processes which regulate carbon assimilation and allocation in tree rings or to relationships with intra-annual environmental variables (Yasue et al., 2000; Ziaco et al., 2016) rather than to limiting factors exerted over the entire growing season (Eckstein, 2004; Ziaco et al., 2016). Regarding isotope parameters, Rbar values computed for 10-yr windows are 0.46 ($\delta^{13}C$) and 0.48 ($\delta^{18}O$).

295 **3.2 Climate-growth relationships**

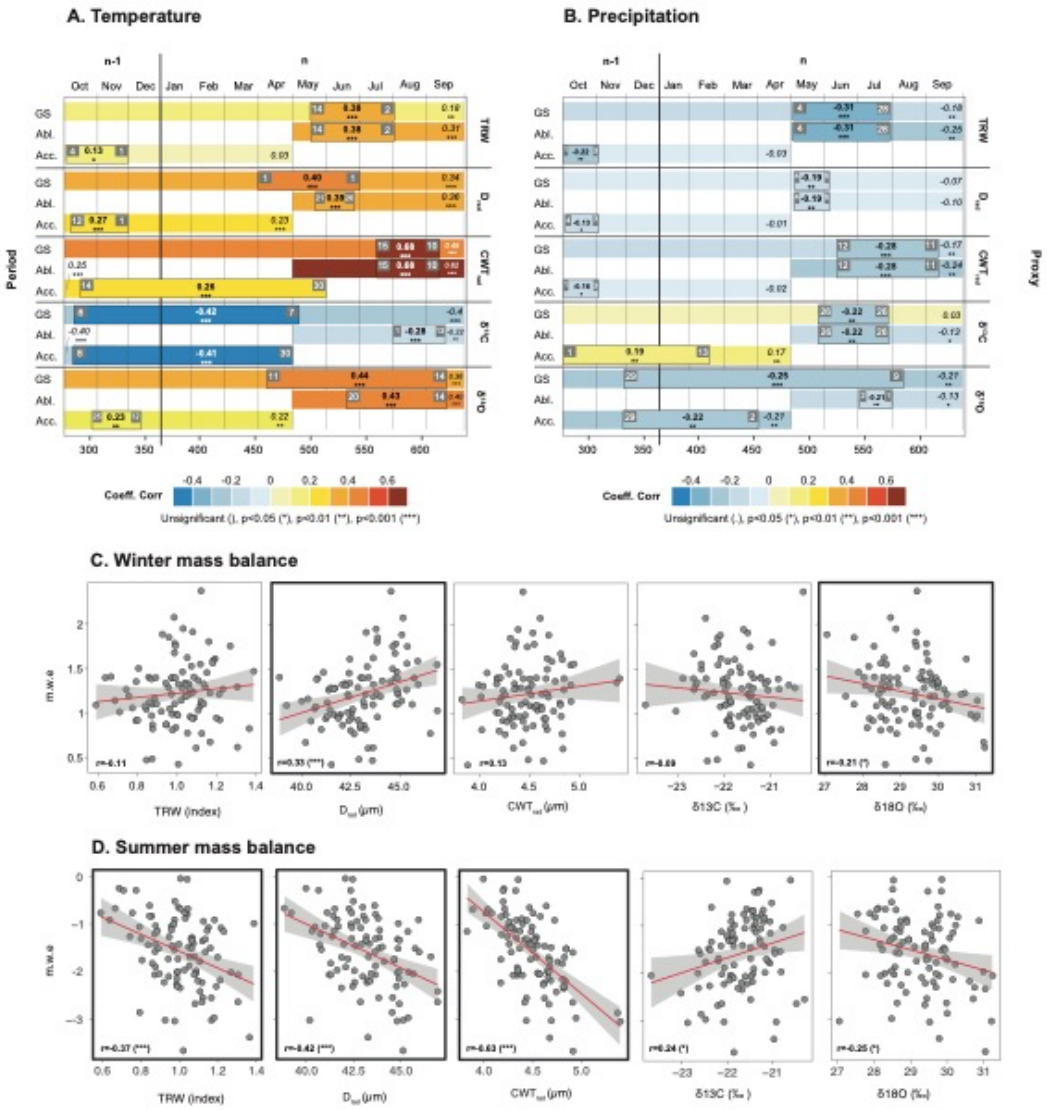

Figure 3. *Correlations between the TRW, D_{rad}, CWT_{rad}, $\delta^{13}C$ and $\delta^{18}O$ chronologies from God da Tamangur, gridded temperature (A) and precipitation (B) fields from Imfeld23, as well as winter (C) and summer (D) mass balance series from the Silvretta glacier. In panels A, B, correlation coefficients and their associated p-values are*
300 *presented in italics for the growing (GS, Oct 1 (n-1)-Sep 30(n)), ablation (Abl, May 1 (n)-Sep 30(n)), and accumulation (Acc, Oct 1 (n-1)-Apr 30 (n)) seasons. Time periods with the highest coefficients (highlighted in bold)*

are delineated by black rectangles. The beginning and end of these optimal periods are denoted by white numbers on a grey background.

Correlation coefficients between the TRW chronology from God da Tamangur and the gridded temperature and precipitation fields from *Imfeld23* show that spring-to-summer temperature is the main driver of radial growth (r_{max}= 0.38, p<0.001; May 14-August 2) between 1802 and 2017 CE (Fig. 3A). For wood anatomical parameters, significant correlations exist between radial diameter (D_{rad}) and early spring to early summer temperatures (r=0.40, p<0.001; April 1 – July 1). This association spans a longer seasonal-window than the ones reported by Carrer et al. (2017, 2018) for earlywood cell areas of *P. cembra* and *P. abies* trees in the Italian Alps. In these studies, correlations were restricted to mid-May/early June and mid-June/mid-July, respectively. At God da Tamangur, highest correlations were obtained between the CWT_{rad} chronology and temperatures over a 58-day time window extending from July 15 to September 10 (r=0.68; p<0.001, Fig. 2). R values computed between CWT_{rad} and summer temperatures agree with results reported by Carrer et al. (2018) for the Italian Dolomites (r>0.6 with July 15–August 15 temperature; 1926–2014) or Știrbu et al. (2022) for the Carpathians (r=0.65 with July-August temperatures; 1961–2013). The period overlaps with the wall-thickening phase observed in latewood during summer for high elevation *P. abies* trees (Gindl et al., 2001; Rossi et al., 2008). Its duration also agrees with current knowledge on xylogenesis, which can last from 1 (mild environments) to 2 months (cold environments) in latewood cells (Rossi et al., 2008; Cuny et al., 2013; Castagneri et al., 2017).

The $\delta^{13}C$ chronologies are negatively correlated with mean daily temperature from October (n-1) to September (n) (r=-0.4, p<0.001) and especially from October 8 (n-1) to May 7 (n) (r=-0.42, p<0.001) (Fig. 3A). Mean daily temperatures from October (n-1) to September (n) (r=0.36, p<0.001) and during the growing season (April 11-September 14, r=0.44, p<0.001) are the main drivers of $\delta^{18}O$ variations. A negative correlation is also found between $\delta^{13}C$ and May 26–July 26 (n) (r=-0.22, p<0.01) and between $\delta^{18}O$ and fall (n-1) to summer (n) precipitation totals (r=-0.25, p<0.01) (Fig.3B). Both chronologies also portray a significant association with winter precipitation (October (n-1)-April (n)), positive for $\delta^{13}C$ (r=0.17, p<0.01), and negative for $\delta^{18}O$ (r=-0.21, p<0.01).

The analysis of $\delta^{13}C$ and $\delta^{18}O$ stable isotope signals in *P. cembra* trees has been initiated only recently in the Alps (Haupt et al., 2014; Arosio et al., 2020) and in the Carpathians (Nagavciuc et al., 2021, 2022; Kern et al., 2023). In the Alps, studies have focused on the detection of age-related trends in the series (Arosio et al., 2020) but did not provide correlation profiles with climatic variables. In the Carpathians, by contrast, positive correlations were reported with April-August temperatures $\delta^{18}O$ (Nagavciuc et al., 2021), in line with our results. By contrast, no significant correlation was found between $\delta^{13}C$ and temperature. Consistent results are also found with precipitation for $\delta^{13}C$, both in Tamangur and Carpathian chronologies which show a negative correlation with June precipitation. The winter signal embedded in the $\delta^{18}O$ chronologies of God da Tamangur echoes the significant associations observed between isotope series and winter precipitation in the Arctic (Holzkämper et al., 2008), Kazakhstan (Qin

et al., 2022) , the Tibetan Plateau, northwestern China (Grießinger et al., 2017; Wernicke et al., 2017; Liu et al., 2013; Qin et al., 2015), Iran (Foroozan et al., 2020) or Pakistan (Treydte et al., 2006) and are thus interpreted as the result of the trees' use of precipitation from before the growing seasons stored in the soil or in groundwater reservoirs. In the Russian Arctic, Holzkämper and Kuhry (2009) suggested that the thickness of the snowpack and the timing of snowmelt has a strong impact on the $\delta^{18}O$ composition of tree-ring α-cellulose because moisture in the early summer is most critical for wood formation. Soil and atmospheric droughts caused by a deficit in previous winter alpine snowfall therefore lead to $\delta^{18}O$ enrichment in tree-ring α-cellulose.

3.3 Multi-proxy glacier mass balance reconstruction

Based on the above climate–growth relation analyses, we tested several combinations of parameters to reconstruct winter (B_w) and summer (B_s) glacier mass balances. The isotopic parameter $\delta^{13}C$ has been excluded from the combinations for B_w and B_s reconstruction because statistically, it is not significant. Statistics of these reconstructions are reported in Tab. 3.

Glacier Mass Balance	Wood proxies	RMSE	r2	RE	CE
Winter Mass Balance (Bw)	Drad	[343.22-353.31] 345.38	[0.03-0.2] 0.1	[-0.12-0.16] 0.08	[-0.23-0.14] 0.04
	δ18O	[350.47-359.87] 352.44	[0.01-0.14] 0.06	[-0.10-0.10] 0.04	[-0.21-0.08] -0.001
	δ18O - Drad	[335.45-347.15] **338.47**	[0.07-0.25] **0.15**	[-0.11-0.20] **0.08**	[-0.22-0.18] **0.06**
Summer Mass Balance (Bs)	TRW	[701.07-721.41] 705.59	[0.05-0.26] 0.14	[-0.1-0.23] 0.12	[-0.19-0.20] 0.07
	Drad	[685.76-706.51] 690.2	[0.07-0.29] 0.17	[-0.08-0.27] 0.16	[-0.16-0.25] 0.12
	CWTrad	[585.93-602.33] 589.35	[0.28-0.51] 0.38	[0.18-0.51] 0.37	[0.12-0.5] 0.35
	δ18O	[728.86-755.31] 734.63	[0.01-0.18] 0.07	[-0.19-0.12] 0.04	[-0.29-0.1] -0.002
	TRW - Drad	[669.76-699.32] 677.34	[0.12-0.34] 0.16	[-0.09-0.3] 0.16	[-0.18-0.27] 0.12
	TRW - CWTrad	[555.33-576.75] 560.95	[0.35-0.58] 0.47	[0.21-0.56] 0.43	[0.15-0.55] 0.4
	TRW - δ18O	[689.24-719.44] 697.43	[0.08-0.31] 0.18	[-0.16-0.25] 0.11	[-0.25-0.23] 0.07
	Drad - CWTrad	[584.24-606.58] 589.88	[0.29-0.53] 0.41	[0.14-0.52] 0.35	[0.08-0.5] 0.33
	Drad - δ18O	[657.71-687.24] 665.3	[0.15-0.38] 0.25	[-0.07-0.33] 0.19	[-0.15-0.31] 0.15
	CWTrad - δ18O	[584.65-609.98] 591.26	[0.30-0.52] 0.41	[0.11-0.5] 0.34	[0.08-0.48] 0.32
	CWTrad - TRW - Drad	[471.23-601.00] **537.12**	[0.37-0.6] **0.49**	[0.19-0.57] **0.43**	[0.14-0.55] **0.4**

Table 3. *Statistics of summer (B_s) and winter (B_w) mass balance reconstructions based on several combinations of tree-ring proxies.*

For the winter mass balance B_w, the best combination includes D_{rad} and $\delta^{18}O$. Both proxies are sensitive to precipitation during the accumulation period and show significant positive (D_{rad}, r=0.33, p<0.001) and negative ($\delta^{18}O$, r=-0.21, p<0.05) correlation with winter mass balance series recorded at Silvretta glacier (Fig. 3C). Both parameters allow a statistically significant reconstruction (RE=0.08, CE=0.06) over the period 1920-2017 (Tab. 3, Fig. 4A) covered by glaciological measurements and tree-proxy reconstructions. At decadal timescales, the 11 yr-spline smoothed winter mass balance reconstructions correlate at 0.65 with observations and capture positive (i.e., from the late 1940s to the late 1950s) and negative (i.e., from the 1960s to 1980s) anomalies over the entire period (Fig. 4A).

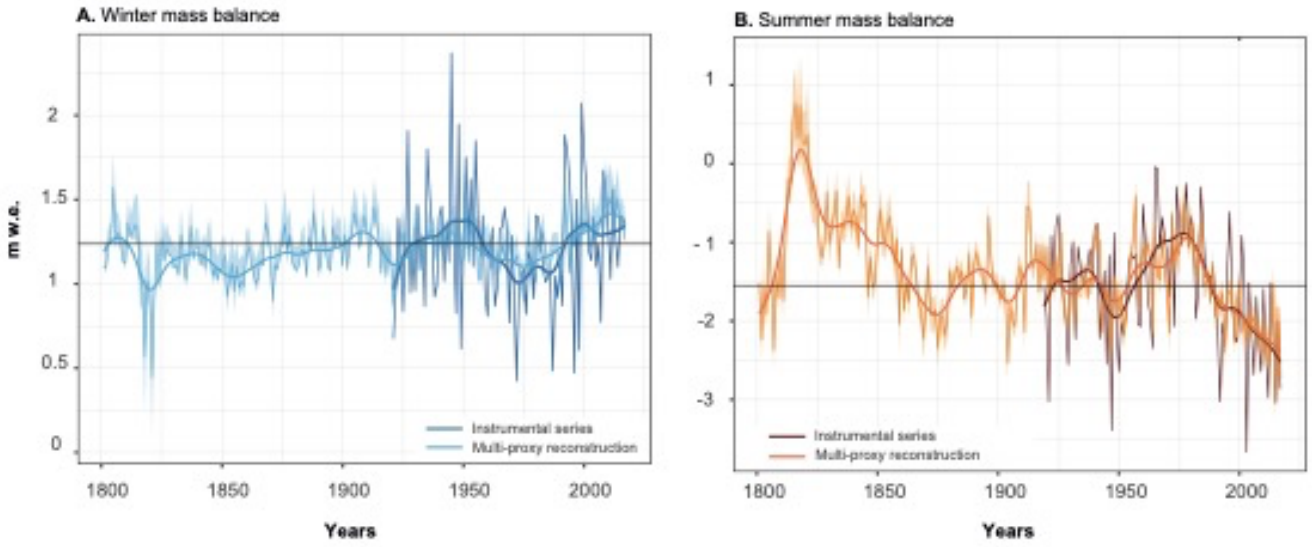

Figure 4. *Winter (A) and summer (B) mass balance of Silvretta glacier reconstructed from tree-ring proxies over the 1802-2017 period. The thin light blue and orange curves illustrate interannual variations in winter and summer mass balance, respectively, derived from $\delta^{18}O$ and D_{rad} (winter) and TRW, CWT_{rad} and D_{rad} (summer). The dark blue and dark brown curves represent the winter and summer mass balance records of Silvretta glacier from 1919-2017. Thick lines indicate decadal variations, smoothed with an 11-year spline. The black line represents the mean of the Winter (A) and summer (B) mass balance reconstructed series.*

The best combination of proxies for summer glacier mass balance B_s includes the TRW, D_{rad} and CWT_{rad} chronologies (Tab. 3, Fig. 3D), each showing significant negative correlations with B_s at -0.37 ($p<0.001$), -0.42 ($p<0.001$) and -0.63 ($p<0.001$), respectively. Based on these proxies, the two first principal components of the principal component regression allow a robust reconstruction of B_s ($r^2=0.49$) and significant RE (0.43 [0.19-0.57]) and CE (0.4, [0.14-0.55]) statistics (Tab. 3). These values exceed those computed by (Cerrato et al., 2020) using *P. cembra* MXD series for Careser glacier over the period 1967-2005 ($r^2=0.45$). The summer balance reconstruction also depicts the positive (1960s to early 1980s) and negative (i.e., 1950s and since the late 1980s) anomalies found in the measurements (Fig. 4B).

Figure 5 shows the 30-yr moving correlations computed between the reconstructed and observed glacier mass balances. Specifically, for winter, it shows a lower correlation for time windows ending between 1981 and 2000, smallest correlations ($r<0.25$) for time windows ending between 1983 and 1999 (Fig. 5A). As this period coincides

with the last phase of positive annual mass balance in the (Southern) Alps (Huss et al. 2015), one can hypothesize that the limited correlations could be related to specific environmental conditions at the site and the complexity of capturing annual glacier mass balance adequately with the tree-ring proxies selected for the B_w reconstruction. In addition, no *in situ* measurements of B_w exist between 1984 and 2003 (Huss and Bauder, 2009) and these gaps in winter mass balance series were filled with a calibrated mass balance model driven by data from nearby meteorological stations (Huss et al., 2015). Therefore, it is also possible that the decrease in correlation may be attributed in part to the quality of the mass balance time series and not result from the tree-proxy dataset.

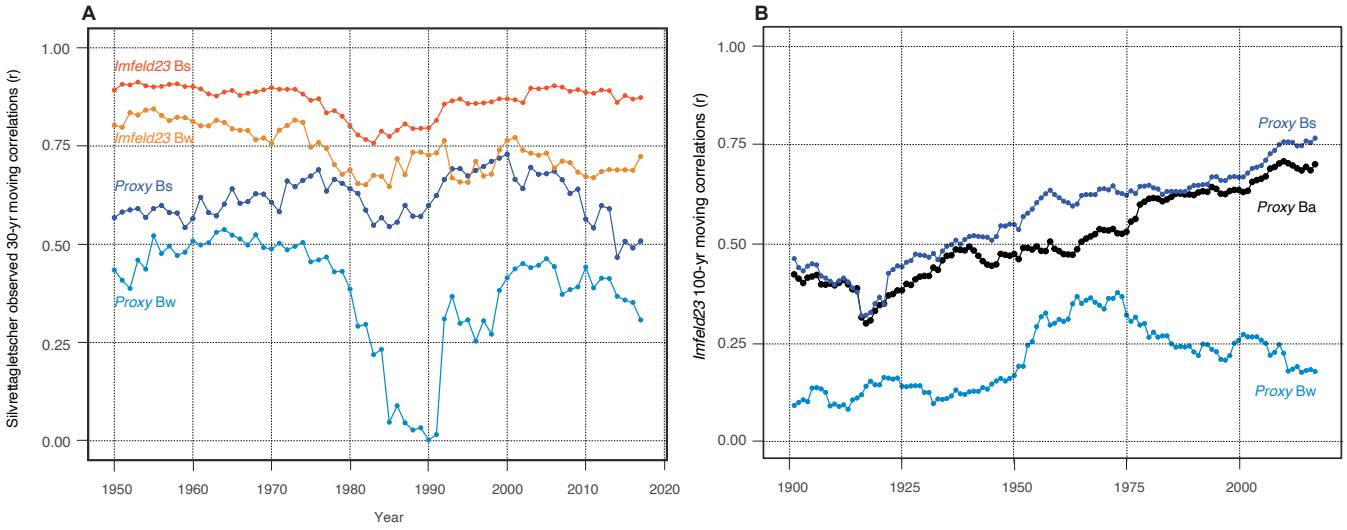

Figure 5. *(A) 30-yr moving correlations (r) of summer (B_s) and winter (B_w) mass balances estimated from gridded temperature and precipitation fields (Imfeld et al., 2023) and multiple wood-proxy B_s and B_w mass balance reconstruction (this study) with the Silvretta glacier B_w and B_s records (Huss et al., 2015). (B) 100-yr moving correlations of proxy B_s, B_w and annual (B_a) mass balance reconstruction with Imfeld23 (Imfeld et al., 2023).*

For B_s, the 30-year correlations between observations and the multi-proxy reconstructions consistently exceed r=0.48 throughout the period covered by the reconstruction, with a limited standard deviation (0.06) between 1920 and 2017 (Fig. 5A). However, while correlation values show an increasing trend (from r=0.52- 0.74) for time windows ending before 2000, they significantly decrease to reach r=0.50 by 2017. This reduction in prediction skills, from r=0.74 to r=0.50, starting in the 1970s, is comparatively less marked than the one documented by Cerrato et al. (2020) (from 0.45 to r=0.2) for *P. cembra*, based on MXD records, albeit occurring a decade earlier. These results confirm that our multiproxy reconstruction records only suffer from limited divergence and standardization issues which notoriously affect both TRW and MXD records but seem to be largely absent in wood anatomical series (Cook et al., 1995; Björklund et al., 2019; Cerrato et al., 2019).

405

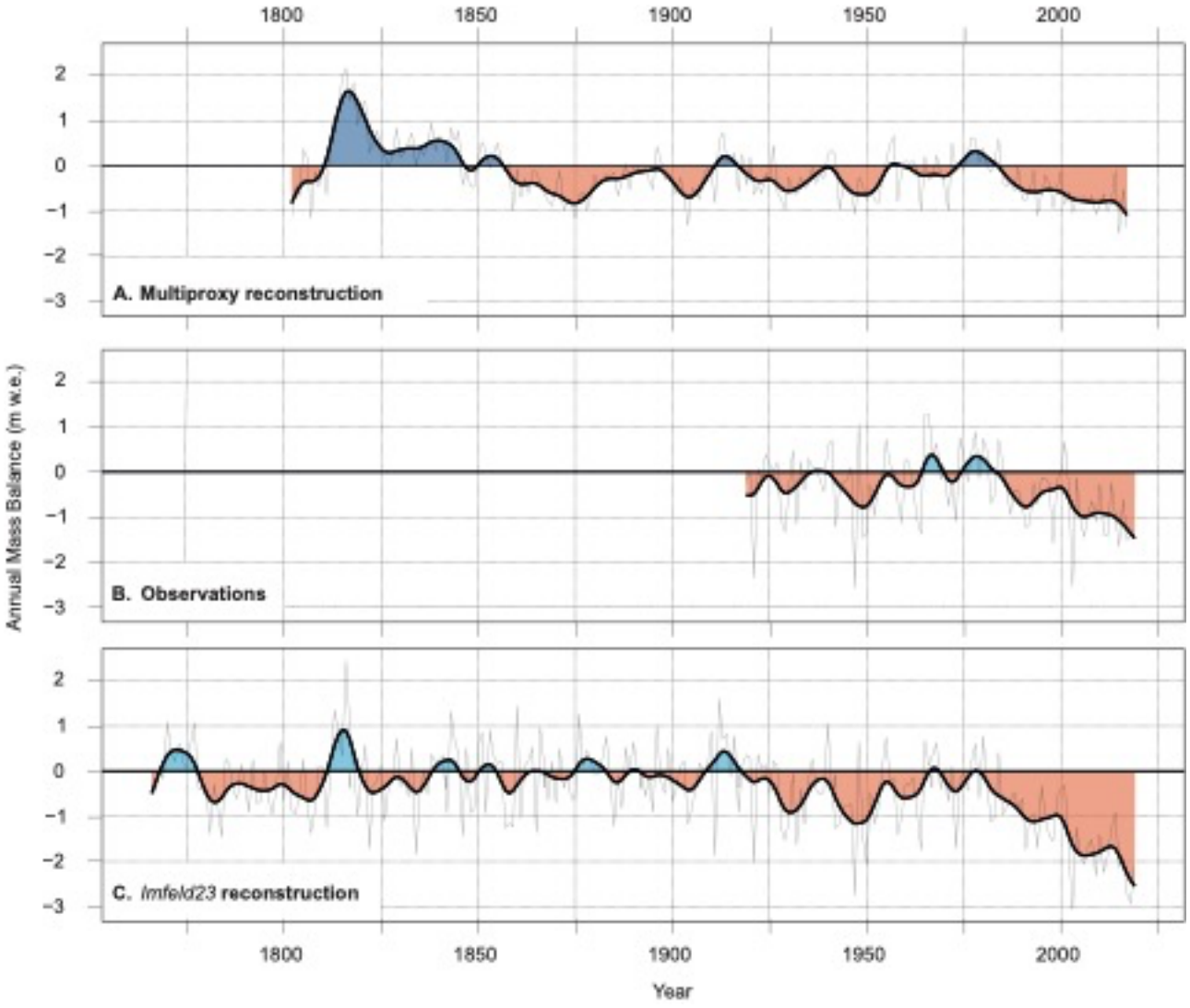

410 **Figure 6.** *Comparison between annual (thin grey lines) and 11-yr spline smoothed (thick lines) variations of (A) the multiple wood-proxy annual mass balance (Ba) reconstruction, (B) observed Ba and (C) Ba reconstructed from gridded temperature and temperature fields (Imfeld et al., 2023). Periods with positive mass balance are shown in blue, periods with negative mass balance are given in red.*

Considering the annual glacier mass balance reconstruction (B_a), we finally combined proxy values for winter and summer balance (Fig. 6A), thus extending the GLAMOS record by 120 years. At interannual timescales, Pearson correlation coefficients between the wood-proxy annual glacier mass balance and *in-situ* measurements at the Silvretta glacier (Fig. 6B) are highly significant at r=0.62 ($p<0.05$). When applying a 11-yr spline to both the reconstructed and measured time series, correlations reach r=0.87. The influence of proxy winter balance on proxy annual balance is limited, explaining only 8% of the annual average variance. These results are consistent with Zemp et al. (2015) for glaciers in the European Alps where winter mass balance explains 6% of the annual mass balance variations on average.

3.4 Comparison with *lmfeld23* records and reconstructions

For the mass balance of the Silvretta glacier, correlations between the observed glacier mass balance and *lmfeld23* are higher than those obtained with the wood proxies. Over the ablation period, lasting from May 1 to September 30, the correlation is r=0.85 ($p<0.001$; 1920–2017) and reaches r=0.87 ($p<0.001$) for the optimal time window extending from May 17 to September 19. Correlations between precipitation from *lmfeld23* and B_w are r=0.48 ($r<0.001$) over the accumulation period *sensu stricto*, from October 1 to April 30, and r=0.49 for the optimal time window extending from October 17 to March 9 (r=0.49, $p<0.001$), respectively. At the annual scale, the *lmfeld23* reconstruction explains 74% of annual glacier mass balance variability observed over the period 1920-2017. Over the full period (1802-2017), the B_s, B_w and B_a wood-proxy reconstructions significantly correlate (r=0.63, 0.15 and 0.61, $p<0.001$) with the reconstruction based on *lmfeld23* (Fig. 6C). Synchronous periods are characterized by positive anomalies in the 1810s, 1840s, 1910s and the late 1970s and likewise, negative anomalies are observed in the two timeseries in the 1870s, the early 20th century, the 1950s and since the mid-1980s. This is well in line with contemporary and documentary sources as well as information on dated moraines available for the Swiss Alps (e.g., Zumbühl et al., 2008; Nussbaumer and Zumbühl, 2012; Schimmelpfennig et al., 2014). More interestingly, the proxy reconstruction shows a strong glacier mass increase in the first part of the 19th century and confirms the abrupt mass loss previously reported in the Alps in the 1850s and 1860s considered to correspond to the end of the Little Ice Age (Holzhauser et al., 2005; Vincent, 2005; Zemp et al., 2006; Painter et al., 2013). Sigl et al. (2015, 2018) hypothesized that the mass gain in the Alps in the early 19th century could result from the strong negative radiative forcing induced by at least five large tropical eruptions between 1809 and 1835 (Sigl et al., 2015; Toohey and Sigl, 2017) in tandem with the Dalton solar minimum (Usoskin et al., 2013; Jungclaus et al., 2017).

By contrast to the wood-proxy reconstruction, this positive annual mass balance pattern is not reproduced by the *lmfeld23* reconstruction and, therefore, the moving correlations computed for 100-yr time periods between both records thus decrease significantly before the 1960s (Fig. 5B). One could hypothesize that this divergence during preindustrial times between the two reconstructions could be attributed (i) to tree-ring proxy, particularly their

reduced explanatory power in colder periods as evidenced for time windows ending between 1983 and 1999 (see §3.3). The divergence could also stem (ii) from the optimal fixed-length window utilized in the *Imfeld23* reconstruction, calibrated on recent environmental conditions. This methodology assumes a constant length for the accumulation and ablation seasons since the early 19th century, despite significant variations in temperature, precipitation, and snowpack conditions compared to the present (Carrer et al., 2023). Such an assumption may introduce bias into the reconstruction (Cerrato et al., 2020). Finally, (iii) the complete absence of high-elevation records in the *Imfeld23* dataset prior to 1864 (see Methods) also raises questions about the robustness of the reconstruction prior to the mid-19th century. It is possible that the gridded temperature and precipitation fields may fail to accurately reproduce changes in winter precipitation distributions in the early stages of their reconstruction.

Conclusions

Mountain glaciers are reliable and unequivocal indicators of climate change due to their sensitivity to changes in temperature and precipitation (Zhang et al., 2019). The advance or retreat of a glacier is thereby related to the amount of snow accumulation as well as snow and ice melt, commonly referred to as its mass balance. This study allowed developing of multi-proxy chronologies from *P. cembra* wood traits based on the dynamic relationships between climate processes that jointly influence tree (cell) growth and glacier mass balance. The Silvretta glacier has been monitored since 1919 and therefore forms a very robust baseline against which the wood-proxy reconstruction presented here can be compared. The study also constitutes an important step in extending glacier mass-balance records beyond the instrumental period for the Swiss Alps. By combining wood anatomical parameters and stable isotopes, we obtain very promising results for seasonal glacier mass balance reconstructions, because some proxies are sensitive to mean temperatures over the entire ablation period while others estimate winter precipitation during the accumulation period. Our results based on multiple wood-proxies reveal that glacier mass gains during the final stages of the Little Ice Age were strongest between 1810 and 1820. Considering the synchronicity of increasing mass balance with a cluster of volcanic eruptions and diminished solar activity, we align with Sigl et al. (2015, 2018) in hypothesizing that these gains may partly result from the co-occurrence of volcanic forcing and the Dalton Minimum. This period of positive mass balances and resulting glacier advances rapidly ended in the 1860s and 1870s when a first episode of substantial negative mass balances led to a first phase of “modern” glacier downwasting.

Competing interests

The contact author has declared that none of the authors has any competing interests.

Acknowledgements

J.L.-S., C.C., and M.S. acknowledge support from the Swiss National Science Foundation (SNSF) Spark project "MNEMOSYNE" and a scnat research grant from the Research Commission of the Swiss National Park (FOK-SNP). C.C., J.L.-S., L.S. and M.S. received funding from the Swiss National Science Foundation (SNSF) Sinergia project CALDERA (no. CRSIIS_183571). We express our gratitude to the reviewers, and especially to Ricardo Cerrato, for their valuable comments, which greatly contributed to improving and clarifying our manuscript.

References

Allen, K. J., Nichols, S. C., Evans, R., and Baker, P. J.: Characteristics of a multi-species conifer network of wood properties chronologies from Southern Australia, Dendrochronologia, 76, 125997, https://doi.org/10.1016/j.dendro.2022.125997, 2022.

Anon: Climate change 2021: the physical science basis : summary for policymakers : working group I contribution to the sixth Assessment report of the Intergovernmental Panel on Climate Change, IPCC, Geneva, Switzerland, 2021.

Arosio, T., Ziehmer, M. M., Nicolussi, K., Schlüchter, C., and Leuenberger, M.: Alpine Holocene tree-ring dataset: age-related trends in the stable isotopes of cellulose show species-specific patterns, Biogeosciences, 17, 4871–4882, https://doi.org/10.5194/bg-17-4871-2020, 2020.

von Arx, G. and Carrer, M.: ROXAS – A new tool to build centuries-long tracheid-lumen chronologies in conifers, Dendrochronologia, 32, 290–293, https://doi.org/10.1016/j.dendro.2013.12.001, 2014.

von Arx, G., Crivellaro, A., Prendin, A. L., Čufar, K., and Carrer, M.: Quantitative Wood Anatomy—Practical Guidelines, Front. Plant Sci., 7, https://doi.org/10.3389/fpls.2016.00781, 2016.

Balanzategui, D., Nordhauß, H., Heinrich, I., Biondi, F., Miley, N., Hurley, A. G., and Ziaco, E.: Wood Anatomy of Douglas-Fir in Eastern Arizona and Its Relationship With Pacific Basin Climate, Front. Plant Sci., 12, 702442, https://doi.org/10.3389/fpls.2021.702442, 2021.

Beaumet, J., Ménégoz, M., Morin, S., Gallée, H., Fettweis, X., Six, D., Vincent, C., Wilhelm, B., and Anquetin, S.: Twentieth century temperature and snow cover changes in the French Alps, Reg Environ Change, 21, 114, https://doi.org/10.1007/s10113-021-01830-x, 2021.

Begert, M., Schlegel, T., and Kirchhofer, W.: Homogeneous temperature and precipitation series of Switzerland from 1864 to 2000, Intl Journal of Climatology, 25, 65–80, https://doi.org/10.1002/joc.1118, 2005.

Björklund, J., Arx, G., Nievergelt, D., Wilson, R., Van den Bulcke, J., Günther, B., Loader, N. J., Rydval, M., Fonti, P., Scharnweber, T., Andreu-Hayles, L., Büntgen, U., D'Arrigo, R., Davi, N., De Mil, T., Esper, J., Gärtner, H., Geary, J., Gunnarson, B. E., Hartl, C., Hevia, A., Song, H., Janecka, K., Kaczka, R. J., Kirdyanov, A. V., Kochbeck, M., Liu, Y., Meko, M., Mundo, I., Nicolussi, K., Oelkers, R., Pichler, T., Sánchez-Salguero, R., Schneider, L., Schweingruber, F., Timonen, M., Trouet, V., Van Acker, J., Verstege, A., Villalba, R., Wilmking, M., and Frank, D.: Scientific Merits and Analytical Challenges of Tree-Ring Densitometry, Rev. Geophys., 57, 1224–1264, https://doi.org/10.1029/2019RG000642, 2019.

Brugnara, Y., Pfister, L., Villiger, L., Rohr, C., Isotta, F. A., and Brönnimann, S.: Early instrumental meteorological observations in Switzerland: 1708–1873, Earth Syst. Sci. Data, 12, 1179–1190, https://doi.org/10.5194/essd-12-1179-2020, 2020.

Brugnara, Y., Hari, C., Pfister, L., Valler, V., and Brönnimann, S.: Pre-industrial temperature variability on the Swiss Plateau derived from the instrumental daily series of Bern and Zurich, Clim. Past, 18, 2357–2379, https://doi.org/10.5194/cp-18-2357-2022, 2022.

Brunetti, M., Maugeri, M., Monti, F., and Nanni, T.: Temperature and precipitation variability in Italy in the last two centuries from homogenised instrumental time series, Int. J. Climatol., 26, 345–381, https://doi.org/10.1002/joc.1251, 2006.

Brunetti, M., Lentini, G., Maugeri, M., Nanni, T., Simolo, C., and Spinoni, J.: Projecting North Eastern Italy temperature and precipitation secular records onto a high-resolution grid, Physics and Chemistry of the Earth, Parts A/B/C, 40–41, 9–22, https://doi.org/10.1016/j.pce.2009.12.005, 2012.

Brunetti, M., Maugeri, M., Nanni, T., Simolo, C., and Spinoni, J.: High-resolution temperature climatology for Italy: interpolation method intercomparison, Intl Journal of Climatology, 34, 1278–1296, https://doi.org/10.1002/joc.3764, 2014.

Brunner, M. I., Farinotti, D., Zekollari, H., Huss, M., and Zappa, M.: Future shifts in extreme flow regimes in Alpine regions, Hydrol. Earth Syst. Sci., 23, 4471–4489, https://doi.org/10.5194/hess-23-4471-2019, 2019.

Bunn, A. G.: A dendrochronology program library in R (dplR), Dendrochronologia, 26, 115–124, https://doi.org/10.1016/j.dendro.2008.01.002, 2008.

Bunn, A. G., Jansma, E., Korpela, M., Westfall, R. D., and Baldwin, J.: Using simulations and data to evaluate mean sensitivity (ζ) as a useful statistic in dendrochronology, Dendrochronologia, 31, 250–254, https://doi.org/10.1016/j.dendro.2013.01.004, 2013.

Büntgen, U., Urban, O., Krusic, P. J., Rybníček, M., Kolář, T., Kyncl, T., Ač, A., Koňasová, E., Čáslavský, J., Esper, J., Wagner, S., Saurer, M., Tegel, W., Dobrovolný, P., Cherubini, P., Reinig, F., and Trnka, M.: Recent European drought extremes beyond Common Era background variability, Nat. Geosci., 14, 190–196, https://doi.org/10.1038/s41561-021-00698-0, 2021.

Carrer, M., Castagneri, D., Prendin, A. L., Petit, G., and von Arx, G.: Retrospective Analysis of Wood Anatomical

Traits Reveals a Recent Extension in Tree Cambial Activity in Two High-Elevation Conifers, Front. Plant Sci., 8, 737, https://doi.org/10.3389/fpls.2017.00737, 2017.

Carrer, M., Unterholzner, L., and Castagneri, D.: Wood anatomical traits highlight complex temperature influence on Pinus cembra at high elevation in the Eastern Alps, Int J Biometeorol, 62, 1745–1753, https://doi.org/10.1007/s00484-018-1577-4, 2018.

Castagneri, D., Fonti, P., von Arx, G., and Carrer, M.: How does climate influence xylem morphogenesis over the growing season? Insights from long-term intra-ring anatomy in *Picea abies*, Ann Bot, mcw274, https://doi.org/10.1093/aob/mcw274, 2017.

Cerrato, R., Salvatore, M. C., Gunnarson, B. E., Linderholm, H. W., Carturan, L., Brunetti, M., and Baroni, C.: *Pinus cembra* L. tree-ring data as a proxy for summer mass-balance variability of the Careser Glacier (Italian Rhaetian Alps), J. Glaciol., 66, 714–726, https://doi.org/10.1017/jog.2020.40, 2020.

Cook, E. R. and Kairiukstis, L. A. (Eds.): Methods of Dendrochronology, Springer Netherlands, Dordrecht, https://doi.org/10.1007/978-94-015-7879-0, 1990.

Cook, E. R., Briffa, K. R., Meko, D. M., Graybill, D. A., and Funkhouser, G.: The "segment length curse" in long tree-ring chronology development for palaeoclimatic studies, The Holocene, 5, 229–237, https://doi.org/10.1177/095968369500500211, 1995.

Coplen, T. B.: New guidelines for reporting stable hydrogen, carbon, and oxygen isotope-ratio data, Geochimica et Cosmochimica Acta, 60, 3359–3360, https://doi.org/10.1016/0016-7037(96)00263-3, 1996.

Crespi, A., Brunetti, M., Lentini, G., and Maugeri, M.: 1961–1990 high-resolution monthly precipitation climatologies for Italy, Intl Journal of Climatology, 38, 878–895, https://doi.org/10.1002/joc.5217, 2018.

Cuny, H. E., Rathgeber, C. B. K., Kiessé, T. S., Hartmann, F. P., Barbeito, I., and Fournier, M.: Generalized additive models reveal the intrinsic complexity of wood formation dynamics, Journal of Experimental Botany, 64, 1983–1994, https://doi.org/10.1093/jxb/ert057, 2013.

Denne, M. P.: Definition of Latewood According to Mork (1928), IAWA J, 10, 59–62, https://doi.org/10.1163/22941932-90001112, 1989.

Dussaillant, I., Berthier, E., Brun, F., Masiokas, M., Hugonnet, R., Favier, V., Rabatel, A., Pitte, P., and Ruiz, L.: Two decades of glacier mass loss along the Andes, Nat. Geosci., 12, 802–808, https://doi.org/10.1038/s41561-019-0432-5, 2019.

Eckstein, D.: Change in past environments – secrets of the tree hydrosystem, New Phytologist, 163, 1–4, https://doi.org/10.1111/j.1469-8137.2004.01117.x, 2004.

Eilmann, B., Weber, P., Rigling, A., and Eckstein, D.: Growth reactions of Pinus sylvestris L. and Quercus pubescens Willd. to drought years at a xeric site in Valais, Switzerland, Dendrochronologia, 23, 121–132, https://doi.org/10.1016/j.dendro.2005.10.002, 2006.

Fonti, P. and García-González, I.: Suitability of chestnut earlywood vessel chronologies for ecological studies, New

Phytologist, 163, 77–86, https://doi.org/10.1111/j.1469-8137.2004.01089.x, 2004.

Foroozan, Z., Grießinger, J., Pourtahmasi, K., and Bräuning, A.: 501 Years of Spring Precipitation History for the Semi-Arid Northern Iran Derived from Tree-Ring δ18O Data, Atmosphere, 11, 889, https://doi.org/10.3390/atmos11090889, 2020.

Francey, R. J., Allison, C. E., Etheridge, D. M., Trudinger, C. M., Enting, I. G., Leuenberger, M., Langenfelds, R. L., Michel, E., and Steele, L. P.: A 1000-year high precision record of δ^{13}C in atmospheric CO_2, Tellus B: Chemical and Physical Meteorology, 51, 170, https://doi.org/10.3402/tellusb.v51i2.16269, 1999.

Fritts, H. C.: Tree rings and climate, Academic Press, London ; New York, 567 pp., 1976.

Gardner, A. S., Moholdt, G., Cogley, J. G., Wouters, B., Arendt, A. A., Wahr, J., Berthier, E., Hock, R., Pfeffer, W. T., Kaser, G., Ligtenberg, S. R. M., Bolch, T., Sharp, M. J., Hagen, J. O., van den Broeke, M. R., and Paul, F.: A Reconciled Estimate of Glacier Contributions to Sea Level Rise: 2003 to 2009, Science, 340, 852–857, https://doi.org/10.1126/science.1234532, 2013.

Gärtner, H. and Schweingruber, F. H.: Microscopic preparation techniques for plant stem analysis, Originalausg., Kessel, Remagen-Oberwinter, 78 pp., 2013.

Gindl, W., Grabner, M., and Wimmer, R.: Effects of altitude on tracheid differentiation and lignification of Norway spruce, Can. J. Bot., 79, 815–821, https://doi.org/10.1139/b01-060, 2001.

Grießinger, J., Bräuning, A., Helle, G., Hochreuther, P., and Schleser, G.: Late Holocene relative humidity history on the southeastern Tibetan plateau inferred from a tree-ring δ 18 O record: Recent decrease and conditions during the last 1500 years, Quaternary International, 430, 52–59, https://doi.org/10.1016/j.quaint.2016.02.011, 2017.

Haupt, M., Friedrich, M., Shishov, V. V., and Boettger, T.: The construction of oxygen isotope chronologies from tree-ring series sampled at different temporal resolution and its use as climate proxies: statistical aspects, Climatic Change, 122, 201–215, https://doi.org/10.1007/s10584-013-0985-z, 2014.

Helama, S., Arppe, L., Timonen, M., Mielikäinen, K., and Oinonen, M.: Age-related trends in subfossil tree-ring δ13C data, Chemical Geology, 416, 28–35, https://doi.org/10.1016/j.chemgeo.2015.10.019, 2015.

Hiemstra, J. F., Young, G. H. F., Loader, N. J., and Gordon, P. R.: Interrogating glacier mass balance response to climatic change since the Little Ice Age: reconstructions for the Jotunheimen region, southern Norway, Boreas, 51, 350–363, https://doi.org/10.1111/bor.12562, 2022.

Hock, R. and Huss, M.: Glaciers and climate change, in: Climate Change, Elsevier, 157–176, https://doi.org/10.1016/B978-0-12-821575-3.00009-8, 2021.

Hoelzle, M., Haeberli, W., Dischl, M., and Peschke, W.: Secular glacier mass balances derived from cumulative glacier length changes, Global and Planetary Change, 36, 295–306, https://doi.org/10.1016/S0921-8181(02)00223-0, 2003.

Holzhauser, H., Magny, M., and Zumbuühl, H. J.: Glacier and lake-level variations in west-central Europe over the last 3500 years, The Holocene, 15, 789–801, https://doi.org/10.1191/0959683605hl853ra, 2005.

Holzkämper, S. and Kuhry, P.: Stable isotopes in tree rings from the Russian Arctic—a proxy for winter precipitation?, PAGES News, 14–15, 2009.

Holzkämper, S., Kuhry, P., Kultti, S., Gunnarson, B., and Sonninen, E.: Stable Isotopes in Tree Rings as Proxies for Winter Precipitation Changes in the Russian Arctic over the Past 150 Years, Geochronometria, 32, 37–46, https://doi.org/10.2478/v10003-008-0025-6, 2008.

Hughes, M. K., Swetnam, T. W., and Diaz, H. F. (Eds.): Dendroclimatology: Progress and Prospects, Springer Netherlands, Dordrecht, https://doi.org/10.1007/978-1-4020-5725-0, 2011.

Huss, M., Bauder, A., Funk, M., and Hock, R.: Determination of the seasonal mass balance of four Alpine glaciers since 1865, J. Geophys. Res., 113, F01015, https://doi.org/10.1029/2007JF000803, 2008.

Huss, M., Bauder, A., and Funk, M.: Homogenization of long-term mass-balance time series, Ann. Glaciol., 50, 198–206, https://doi.org/10.3189/172756409787769627, 2009.

Huss, M., Dhulst, L., and Bauder, A.: New long-term mass-balance series for the Swiss Alps, J. Glaciol., 61, 551–562, https://doi.org/10.3189/2015JoG15J015, 2015.

Huss, M., Bauder, A., Linsbauer, A., Gabbi, J., Kappenberger, G., Steinegger, U., and Farinotti, D.: More than a century of direct glacier mass-balance observations on Claridenfirn, Switzerland, J. Glaciol., 67, 697–713, https://doi.org/10.1017/jog.2021.22, 2021.

Imfeld, N., Pfister, L., Brugnara, Y., and Brönnimann, S.: 250 years of daily weather: Temperature and precipitation fields for Switzerland since 1763, Atmospheric Dynamics/Historical Records/Instrumental Period, https://doi.org/10.5194/egusphere-2022-1140, 2022.

Imfeld, N., Pfister, L., Brugnara, Y., and Brönnimann, S.: A 258-year-long data set of temperature and precipitation fields for Switzerland since 1763, Clim. Past, 19, 703–729, https://doi.org/10.5194/cp-19-703-2023, 2023.

Ipcc: The Ocean and Cryosphere in a Changing Climate: Special Report of the Intergovernmental Panel on Climate Change, 1st ed., Cambridge University Press, https://doi.org/10.1017/9781009157964, 2022.

Jevšenak, J. and Levanič, T.: dendroTools: R package for studying linear and nonlinear responses between tree-rings and daily environmental data, Dendrochronologia, 48, 32–39, https://doi.org/10.1016/j.dendro.2018.01.005, 2018.

Jungclaus, J. H., Bard, E., Baroni, M., Braconnot, P., Cao, J., Chini, L. P., Egorova, T., Evans, M., González-Rouco, J. F., Goosse, H., Hurtt, G. C., Joos, F., Kaplan, J. O., Khodri, M., Klein Goldewijk, K., Krivova, N., LeGrande, A. N., Lorenz, S. J., Luterbacher, J., Man, W., Maycock, A. C., Meinshausen, M., Moberg, A., Muscheler, R., Nehrbass-Ahles, C., Otto-Bliesner, B. I., Phipps, S. J., Pongratz, J., Rozanov, E., Schmidt, G. A., Schmidt, H., Schmutz, W., Schurer, A., Shapiro, A. I., Sigl, M., Smerdon, J. E., Solanki, S. K., Timmreck, C., Toohey, M., Usoskin, I. G., Wagner, S., Wu, C.-J., Yeo, K. L., Zanchettin, D., Zhang, Q., and Zorita, E.: The PMIP4 contribution to CMIP6 – Part 3: The last millennium, scientific objective, and experimental design for the PMIP4 <i>past1000</i> simulations, Geosci. Model Dev., 10, 4005–4033, https://doi.org/10.5194/gmd-10-4005-

2017, 2017.

Kern, Z., Nagavciuc, V., Hatvani, I. G., Hegyi, I. N., Loader, N. J., and Popa, I.: Evaluation of the non-climatic (age-related) trends of stable oxygen and carbon isotopes in Swiss stone pine (Pinus cembra L.) tree rings from the Eastern Carpathians, Romania, Dendrochronologia, 78, 126061, https://doi.org/10.1016/j.dendro.2023.126061, 2023.

Kinnard, C., Larouche, O., Demuth, M. N., and Menounos, B.: Modelling glacier mass balance and climate sensitivity in the context of sparse observations: application to Saskatchewan Glacier, western Canada, The Cryosphere, 16, 3071–3099, https://doi.org/10.5194/tc-16-3071-2022, 2022.

Larocque, S. J. and Smith, D. J.: 'Little Ice Age' proxy glacier mass balance records reconstructed from tree rings in the Mt Waddington area, British Columbia Coast Mountains, Canada, The Holocene, 15, 748–757, https://doi.org/10.1191/0959683605hl848rp, 2005.

Leavitt, S. W. and Danzer, S. R.: Method for batch processing small wood samples to holocellulose for stable-carbon isotope analysis, Anal. Chem., 65, 87–89, https://doi.org/10.1021/ac00049a017, 1993.

Lewis, D. and Smith, D.: Dendrochronological Mass Balance Reconstruction, Strathcona Provincial Park, Vancouver Island, British Columbia, Canada, Arctic, Antarctic, and Alpine Research, 36, 598–606, https://doi.org/10.1657/1523-0430(2004)036[0598:DMBRSP]2.0.CO;2, 2004.

Liang, W., Heinrich, I., Simard, S., Helle, G., Linan, I. D., and Heinken, T.: Climate signals derived from cell anatomy of Scots pine in NE Germany, Tree Physiology, 33, 833–844, https://doi.org/10.1093/treephys/tpt059, 2013.

Linderholm, H. W., Jansson, P., and Chen, D.: A high-resolution reconstruction of Storglaciären mass balance back to 1780/81 using tree-ring data and circulation indices, Quat. res., 67, 12–20, https://doi.org/10.1016/j.yqres.2006.08.005, 2007.

Liu, W., Li, X., An, Z., Xu, L., and Zhang, Q.: Total organic carbon isotopes: A novel proxy of lake level from Lake Qinghai in the Qinghai–Tibet Plateau, China, Chemical Geology, 347, 153–160, https://doi.org/10.1016/j.chemgeo.2013.04.009, 2013.

Lopez-Saez, J., Corona, C., von Arx, G., Fonti, P., Slamova, L., and Stoffel, M.: Tree-ring anatomy of Pinus cembra trees opens new avenues for climate reconstructions in the European Alps, Science of The Total Environment, 855, 158605, https://doi.org/10.1016/j.scitotenv.2022.158605, 2023.

Malcomb, N. L. and Wiles, G. C.: Tree-ring-based reconstructions of North American glacier mass balance through the Little Ice Age — Contemporary warming transition, Quat. res., 79, 123–137, https://doi.org/10.1016/j.yqres.2012.11.005, 2013.

Marzeion, B., Kaser, G., Maussion, F., and Champollion, N.: Limited influence of climate change mitigation on short-term glacier mass loss, Nature Clim Change, 8, 305–308, https://doi.org/10.1038/s41558-018-0093-1, 2018.

McCarroll, D. and Loader, N. J.: Stable isotopes in tree rings, Quaternary Science Reviews, 23, 771–801, https://doi.org/10.1016/j.quascirev.2003.06.017, 2004.

Nagavciuc, V., Bădăluţă, C.-A., and Ionita, M.: The influence of the Carpathian Mountains on the variability of stable isotopes in precipitation and the relationship with large-scale atmospheric circulation, SP, 507, 19–46, https://doi.org/10.1144/SP507-2020-69, 2021.

Nagavciuc, V., Ionita, M., Kern, Z., McCarroll, D., and Popa, I.: A ~700 years perspective on the 21st century drying in the eastern part of Europe based on δ18O in tree ring cellulose, Commun Earth Environ, 3, 277, https://doi.org/10.1038/s43247-022-00605-4, 2022.

Nemec, J., Huybrechts, P., Rybak, O., and Oerlemans, J.: Reconstruction of the annual balance of Vadret da Morteratsch, Switzerland, since 1865, Ann. Glaciol., 50, 126–134, https://doi.org/10.3189/172756409787769609, 2009.

Nicolussi, K. and Patzelt, G.: Reconstructing glacier history in Tyrol by means of tree-ring investigations, Zeitschrift Für Gletscherkunde und Galzialgeologie, 207–215, 1996.

Nussbaumer, S. U. and Zumbühl, H. J.: The Little Ice Age history of the Glacier des Bossons (Mont Blanc massif, France): a new high-resolution glacier length curve based on historical documents, Climatic Change, 111, 301–334, https://doi.org/10.1007/s10584-011-0130-9, 2012.

Olano, J. M., Eugenio, M., García-Cervigón, A. I., Folch, M., and Rozas, V.: Quantitative Tracheid Anatomy Reveals a Complex Environmental Control of Wood Structure in Continental Mediterranean Climate, International Journal of Plant Sciences, 173, 137–149, https://doi.org/10.1086/663165, 2012.

Painter, T. H., Flanner, M. G., Kaser, G., Marzeion, B., VanCuren, R. A., and Abdalati, W.: End of the Little Ice Age in the Alps forced by industrial black carbon, Proc. Natl. Acad. Sci. U.S.A., 110, 15216–15221, https://doi.org/10.1073/pnas.1302570110, 2013.

Pfister, L., Hupfer, F., Brugnara, Y., Munz, L., Villiger, L., Meyer, L., Schwander, M., Isotta, F. A., Rohr, C., and Brönnimann, S.: Early instrumental meteorological measurements in Switzerland, Clim. Past, 15, 1345–1361, https://doi.org/10.5194/cp-15-1345-2019, 2019.

Prendin, A. L., Petit, G., Carrer, M., Fonti, P., Björklund, J., and von Arx, G.: New research perspectives from a novel approach to quantify tracheid wall thickness, Tree Physiology, 37, 976–983, https://doi.org/10.1093/treephys/tpx037, 2017.

Pritzkow, C., Heinrich, I., Grudd, H., and Helle, G.: Relationship between wood anatomy, tree-ring widths and wood density of Pinus sylvestris L. and climate at high latitudes in northern Sweden, Dendrochronologia, 32, 295–302, https://doi.org/10.1016/j.dendro.2014.07.003, 2014.

Qin, C., Yang, B., Bräuning, A., Grießinger, J., and Wernicke, J.: Drought signals in tree-ring stable oxygen isotope series of Qilian juniper from the arid northeastern Tibetan Plateau, Global and Planetary Change, 125, 48–59, https://doi.org/10.1016/j.gloplacha.2014.12.002, 2015.

Qin, L., Bolatov, K., Shang, H., Yu, S., Gou, X., Bagila, M., Bolatova, A., Ainur, U., and Zhang, R.: Reconstruction of alpine snowfall in southern Kazakhstan based on oxygen isotopes in tree rings, Theor Appl Climatol, 148, 727–

737, https://doi.org/10.1007/s00704-022-03974-0, 2022.

R Core Team, 2023. R: A Language and Environment for Statistical Computing. R Foundation for Statistical Computing, Vienna, Austria. https://www.R-project.org/., R Foundation for Statistical Computing, Vienna.

Rossi, S., Deslauriers, A., Griçar, J., Seo, J.-W., Rathgeber, C. B., Anfodillo, T., Morin, H., Levanic, T., Oven, P., and Jalkanen, R.: Critical temperatures for xylogenesis in conifers of cold climates, Global Ecology and Biogeography, 17, 696–707, https://doi.org/10.1111/j.1466-8238.2008.00417.x, 2008.

Rounce, D. R., Hock, R., Maussion, F., Hugonnet, R., Kochtitzky, W., Huss, M., Berthier, E., Brinkerhoff, D., Compagno, L., Copland, L., Farinotti, D., Menounos, B., and McNabb, R. W.: Global glacier change in the 21st century: Every increase in temperature matters, Science, 379, 78–83, https://doi.org/10.1126/science.abo1324, 2023.

Saulnier, M., Edouard, J.-L., Corona, C., and Guibal, F.: Climate/growth relationships in a Pinus cembra high-elevation network in the Southern French Alps, Annals of Forest Science, 68, 189–200, https://doi.org/10.1007/s13595-011-0020-3, 2011.

Schimmelpfennig, I., Schaefer, J. M., Akçar, N., Koffman, T., Ivy-Ochs, S., Schwartz, R., Finkel, R. C., Zimmerman, S., and Schlüchter, C.: A chronology of Holocene and Little Ice Age glacier culminations of the Steingletscher, Central Alps, Switzerland, based on high-sensitivity beryllium-10 moraine dating, Earth and Planetary Science Letters, 393, 220–230, https://doi.org/10.1016/j.epsl.2014.02.046, 2014.

Seftigen, K., Fonti, M. V., Luckman, B., Rydval, M., Stridbeck, P., von Arx, G., Wilson, R., and Björklund, J.: Prospects for dendroanatomy in paleoclimatology – a case study on <i>Picea engelmannii</i> from the Canadian Rockies, Clim. Past, 18, 1151–1168, https://doi.org/10.5194/cp-18-1151-2022, 2022.

Sigl, M., Winstrup, M., McConnell, J. R., Welten, K. C., Plunkett, G., Ludlow, F., Büntgen, U., Caffee, M., Chellman, N., Dahl-Jensen, D., Fischer, H., Kipfstuhl, S., Kostick, C., Maselli, O. J., Mekhaldi, F., Mulvaney, R., Muscheler, R., Pasteris, D. R., Pilcher, J. R., Salzer, M., Schüpbach, S., Steffensen, J. P., Vinther, B. M., and Woodruff, T. E.: Timing and climate forcing of volcanic eruptions for the past 2,500 years, Nature, 523, 543–549, https://doi.org/10.1038/nature14565, 2015.

Sigl, M., Abram, N. J., Gabrieli, J., Jenk, T. M., Osmont, D., and Schwikowski, M.: 19th century glacier retreat in the Alps preceded the emergence of industrial black carbon deposition on high-alpine glaciers, The Cryosphere, 12, 3311–3331, https://doi.org/10.5194/tc-12-3311-2018, 2018.

Sold, L., Huss, M., Machguth, H., Joerg, P. C., Leysinger Vieli, G., Linsbauer, A., Salzmann, N., Zemp, M., and Hoelzle, M.: Mass Balance Re-analysis of Findelengletscher, Switzerland; Benefits of Extensive Snow Accumulation Measurements, Front. Earth Sci., 4, https://doi.org/10.3389/feart.2016.00018, 2016.

Știrbu, M.-I., Roibu, C.-C., Carrer, M., Mursa, A., Unterholzner, L., and Prendin, A. L.: Contrasting Climate Sensitivity of Pinus cembra Tree-Ring Traits in the Carpathians, Front. Plant Sci., 13, 855003, https://doi.org/10.3389/fpls.2022.855003, 2022.

Stokes, M. A. and Smiley, T. L.: An introduction to tree-ring dating, University of Arizona Press, Tucson, 73 pp., 1996.

Toohey, M. and Sigl, M.: Volcanic stratospheric sulfur injections and aerosol optical depth from 500 BCE to 1900 CE, Earth Syst. Sci. Data, 9, 809–831, https://doi.org/10.5194/essd-9-809-2017, 2017.

Torbenson, M., Klippel, L., Hartl, C., Reinig, F., Treydte, K., Büntgen, U., Trnka, M., Schöne, B., Schneider, L., and Esper, J.: Investigation of age trends in tree-ring stable carbon and oxygen isotopes from northern Fennoscandia over the past millennium, Quaternary International, 631, 105–114, https://doi.org/10.1016/j.quaint.2022.05.017, 2022.

Treydte, K. S., Schleser, G. H., Helle, G., Frank, D. C., Winiger, M., Haug, G. H., and Esper, J.: The twentieth century was the wettest period in northern Pakistan over the past millennium, Nature, 440, 1179–1182, https://doi.org/10.1038/nature04743, 2006.

Usoskin, I. G., Kromer, B., Ludlow, F., Beer, J., Friedrich, M., Kovaltsov, G. A., Solanki, S. K., and Wacker, L.: The AD775 cosmic event revisited: the Sun is to blame, A&A, 552, L3, https://doi.org/10.1051/0004-6361/201321080, 2013.

Vincent, A., Violette, S., and Aðalgeirsdóttir, G.: Groundwater in catchments headed by temperate glaciers: A review, Earth-Science Reviews, 188, 59–76, https://doi.org/10.1016/j.earscirev.2018.10.017, 2019.

Vincent, C.: Solving the paradox of the end of the Little Ice Age in the Alps, Geophys. Res. Lett., 32, L09706, https://doi.org/10.1029/2005GL022552, 2005.

Watson, E., Luckman, B. H., and Yu, B.: Long-term relationships between reconstructed seasonal mass balance at Peyto Glacier, Canada, and Pacific sea surface temperatures, The Holocene, 16, 783–790, https://doi.org/10.1191/0959683606hol973ft, 2006.

Wernicke, J., Hochreuther, P., Grießinger, J., Zhu, H., Wang, L., and Bräuning, A.: Air mass origin signals in δ 18O of tree-ring cellulose revealed by back-trajectory modeling at the monsoonal Tibetan plateau, Int J Biometeorol, 61, 1109–1124, https://doi.org/10.1007/s00484-016-1292-y, 2017.

Wigley, T. M. L., Lough, J. M., and Jones, P. D.: Spatial patterns of precipitation in England and Wales and a revised, homogeneous England and Wales precipitation series, J. Climatol., 4, 1–25, https://doi.org/10.1002/joc.3370040102, 1984.

Wood, L. J., Smith, D. J., and Demuth, M. N.: Extending the Place Glacier mass-balance record to AD 1585, using tree rings and wood density, Quat. res., 76, 305–313, https://doi.org/10.1016/j.yqres.2011.07.003, 2011.

Wouters, B., Gardner, A. S., and Moholdt, G.: Global Glacier Mass Loss During the GRACE Satellite Mission (2002-2016), Front. Earth Sci., 7, 96, https://doi.org/10.3389/feart.2019.00096, 2019.

Yasue, K., Funada, R., Kobayashi, O., and Ohtani, J.: The effects of tracheid dimensions on variations in maximum density of Picea glehnii and relationships to climatic factors, Trees, 14, 223–229, https://doi.org/10.1007/PL00009766, 2000.

Zekollari, H., Huss, M., and Farinotti, D.: Modelling the future evolution of glaciers in the European Alps under the EURO-CORDEX RCM ensemble, The Cryosphere, 13, 1125–1146, https://doi.org/10.5194/tc-13-1125-2019, 2019.

Zemp, M., Haeberli, W., Hoelzle, M., and Paul, F.: Alpine glaciers to disappear within decades?, Geophys. Res. Lett., 33, L13504, https://doi.org/10.1029/2006GL026319, 2006.

Zemp, M., Frey, H., Gärtner-Roer, I., Nussbaumer, S. U., Hoelzle, M., Paul, F., Haeberli, W., Denzinger, F., Ahlstrøm, A. P., Anderson, B., Bajracharya, S., Baroni, C., Braun, L. N., Cáceres, B. E., Casassa, G., Cobos, G., Dávila, L. R., Delgado Granados, H., Demuth, M. N., Espizua, L., Fischer, A., Fujita, K., Gadek, B., Ghazanfar, A., Ove Hagen, J., Holmlund, P., Karimi, N., Li, Z., Pelto, M., Pitte, P., Popovnin, V. V., Portocarrero, C. A., Prinz, R., Sangewar, C. V., Severskiy, I., Sigurđsson, O., Soruco, A., Usubaliev, R., and Vincent, C.: Historically unprecedented global glacier decline in the early 21st century, J. Glaciol., 61, 745–762, https://doi.org/10.3189/2015JoG15J017, 2015.

Zemp, M., Huss, M., Thibert, E., Eckert, N., McNabb, R., Huber, J., Barandun, M., Machguth, H., Nussbaumer, S. U., Gärtner-Roer, I., Thomson, L., Paul, F., Maussion, F., Kutuzov, S., and Cogley, J. G.: Global glacier mass changes and their contributions to sea-level rise from 1961 to 2016, Nature, 568, 382–386, https://doi.org/10.1038/s41586-019-1071-0, 2019.

Zhang, Z., Liu, S., Jiang, Z., Shangguan, D., Wei, J., Guo, W., Xu, J., Zhang, Y., and Huang, D.: Glacier changes and surges over Xinqingfeng and Malan Ice Caps in the inner Tibetan Plateau since 1970 derived from Remote Sensing Data, Glaciers/Remote Sensing, https://doi.org/10.5194/tc-2019-94, 2019.

Ziaco, E., Biondi, F., and Heinrich, I.: Wood Cellular Dendroclimatology: Testing New Proxies in Great Basin Bristlecone Pine, Front. Plant Sci., 7, https://doi.org/10.3389/fpls.2016.01602, 2016.

Zumbühl, H. J., Steiner, D., and Nussbaumer, S. U.: 19th century glacier representations and fluctuations in the central and western European Alps: An interdisciplinary approach, Global and Planetary Change, 60, 42–57, https://doi.org/10.1016/j.gloplacha.2006.08.005, 2008.